

GridVAD: Open-Set Video Anomaly Detection via Spatial Reasoning over Stratified Frame Grids

Mohamed Eltahir^{†1}, Ahmed O. Ibrahim^{*2}, Obada Siralkhatim^{*2},
Tabarak Abdallah², and Sondos Mohamed^{‡3}

¹ King Abdullah University of Science and Technology (KAUST), Thuwal, Saudi Arabia

`mohamed.hamid@kaust.edu.sa`

² Independent Researcher

`{ahmed.o.a.ibrahim, obadabadee.pro, tabarak.m.elgady}@gmail.com`

³ National Center for Research (NCR), Khartoum, Sudan

`Sondos.Mohamed@ncr.gov.sd`

Abstract. Vision-Language Models (VLMs) are powerful open-set reasoners, yet their direct use as anomaly detectors in video surveillance is fragile: without calibrated anomaly priors, they alternate between missed detections and hallucinated false alarms. We argue the problem is not the VLM itself but how it is used. VLMs should function as *anomaly proposers*, generating open-set candidate descriptions that are then grounded and tracked by purpose-built spatial and temporal modules. We instantiate this *propose-ground-propagate* principle in **GridVAD**, a training-free pipeline that produces pixel-level anomaly masks without any domain-specific training. A VLM reasons over stratified grid representations of video clips to generate natural-language anomaly proposals. Self-Consistency Consolidation (SCC) filters hallucinations by retaining only proposals that recur across multiple independent samplings. Grounding DINO anchors each surviving proposal to a bounding box, and SAM2 propagates it as a dense mask through the anomaly interval. The per-clip VLM budget is fixed at $M+1$ calls regardless of video length, where M can be set according to the proposals needed. On UCSD Ped2, GridVAD achieves the highest Pixel-AUROC (77.59) among all compared methods, surpassing even the partially fine-tuned TAO (75.11), and outperforms other zero-shot approaches on object-level RBDC by over $5\times$. Ablations reveal that SCC provides a controllable precision-recall tradeoff: filtering improves all pixel-level metrics at a modest cost in object-level recall. Efficiency experiments show GridVAD is $2.7\times$ more call-efficient than uniform per-frame VLM querying while additionally producing dense segmentation masks. Code and qualitative video results are available at <https://gridvad.github.io>.

Keywords: Video Anomaly Detection, Zero-Shot, Vision-Language Models, VLM, GridVAD, Open-Set Reasoning.

1 Introduction

Video Anomaly Detection (VAD) aims to detect and temporally localize events that deviate from established scene dynamics [9]. Unlike closed-set action recognition, VAD is an inherently unbalanced, open-set problem, where anomalies are characterized by their rarity, diversity, and extreme context-dependency [29]. For instance, while running is considered a pedestrian regularity on a sidewalk, it may signify a critical security deviation within a restricted industrial facility. These properties make VAD particularly resistant to closed-vocabulary, distribution-fitting approaches, and have recently motivated the use of foundation models as a more flexible alternative. Despite these challenges, VAD remains indispensable in safety critical deployments including autonomous driving [3], public transportation monitoring and industrial surveillance [22] where reliable detection of anomalous events is essential to mitigate potential risks.

Vision-Language Models (VLMs) appear ideally suited for VAD: they possess broad visual knowledge, can reason about novel event categories, and produce natural-language descriptions that are inherently interpretable. Early work (*LAVAD* [29], *SUVAD* [5]) has demonstrated impressive zero-shot temporal detection using VLM-derived frame scores. Yet these methods share a common design choice: the VLM or LLM is directly employed to score individual frames or clips for anomaly probability. This design is fragile. VLMs and

* Equal Contribution † Corresponding Author ‡ Supervising Author

LLMs are trained on internet-scale data where anomalous events are neither rare nor systematically labeled, so their anomaly scores are not calibrated. The same model that correctly flags a vehicle in a pedestrian zone may also flag a person running, a shadow, or an empty scene, with comparable confidence. The result is a noisy signal that requires extensive post-processing to be actionable.

We propose that the correct role for a VLM in a VAD pipeline is not detection but *proposal*: generating open-set natural-language descriptions of candidate anomalous events, without being required to make a calibrated binary decision. This separates two sub-problems that should not be conflated. The VLM handles what it does well: recognizing and describing unusual visual content in open vocabulary. Spatial grounding and temporal localization are then handled by purpose-built models (Grounding DINO [13], SAM2 [20]) that are designed for precise spatial reasoning. Reliability comes not from asking the VLM to be more accurate, but from filtering its outputs statistically: proposals that recur across multiple independent samplings of the same clip are retained, while one-off hallucinations are discarded.

We instantiate this *propose-ground-propagate* principle in **GridVAD**, a training-free pipeline. A video clip is represented as a stratified spatial grid of frame samples, converting the temporal detection problem into a single-pass image understanding task. The VLM generates free-form anomaly proposals with temporal coordinates. A Self-Consistency Consolidation (SCC) stage semantically deduplicates proposals across M independent grid samplings, retaining only those with cross-sampling support above a threshold. Grounding DINO anchors each surviving proposal to a bounding box in the most informative frame, and SAM2 propagates it as a per-frame mask through the proposed interval. No component is trained on anomaly data. The pipeline is budget-controlled: regardless of video length, it requires exactly $M+1$ VLM calls per clip.

Experiments on *UCSD Ped2* [17] and *ShanghaiTech Campus* [14] validate this decomposition. On UCSD Ped2, **GridVAD** achieves the highest Pixel-AUROC (77.59) among all compared methods, surpassing the partially fine-tuned TAO [9] (75.11), and outperforms other zero-shot approaches on object-level RBDC by over $5\times$, all without any dataset-specific fine-tuning or closed-set category lists. Ablations reveal a controllable precision-recall tradeoff governed by SCC, and efficiency experiments show GridVAD is $2.7\times$ more call-efficient than uniform per-frame VLM querying.

Contributions.

- We identify and articulate the **VLM-as-proposer design principle**: VLMs used as direct anomaly detectors produce noisy, uncalibrated outputs, but when repositioned as open-set proposers within a propose-ground-propagate decomposition, they enable reliable pixel-level anomaly localization without any task-specific training.
- We introduce **Self-Consistency Consolidation (SCC)**, a lightweight hallucination filtering mechanism that treats the VLM as a stochastic sensor and retains only proposals with cross-sampling statistical support, requiring no learned parameters and no dataset-specific calibration. We show empirically that SCC controls a precision-recall tradeoff between pixel-level mask quality and object-level detection recall.
- We propose the **stratified grid representation**, which converts temporal anomaly detection into a single-pass spatial reasoning task, enabling budget-controlled VLM querying that is independent of video length and $2.7\times$ more call-efficient than per-frame alternatives.

2 Related Work

Training-based VAD. The dominant paradigm in VAD trains models to recognize normality and flag deviations, spanning fully supervised [2, 12, 25], weakly supervised [11, 23, 26, 32], and one-class settings [8, 15, 24, 27]. While effective within their target domains, these methods require annotated data or clean normality distributions, and they generalize poorly to anomaly categories not seen during training. Object-centric approaches [6, 10, 21] improve spatial precision by grounding anomaly scores in detected objects, but remain bound to fixed detection vocabularies and per-dataset tuning.

VLMs as direct anomaly detectors. Large Vision-Language Models (VLMs) have sparked interest in training-free VAD by enabling open-set semantic reasoning without distribution-fitting. *LAVAD* [29] scores individual frames by comparing VLM-generated captions against a normal-event reference, producing frame-level anomaly signals. *SUVAD* [5] generates textual prototypes of normal and abnormal events, then scores frames by comparing per-frame captions via an LLM. *Holmes-VAD* [31] and *VERA* [28] partially fine-tune or

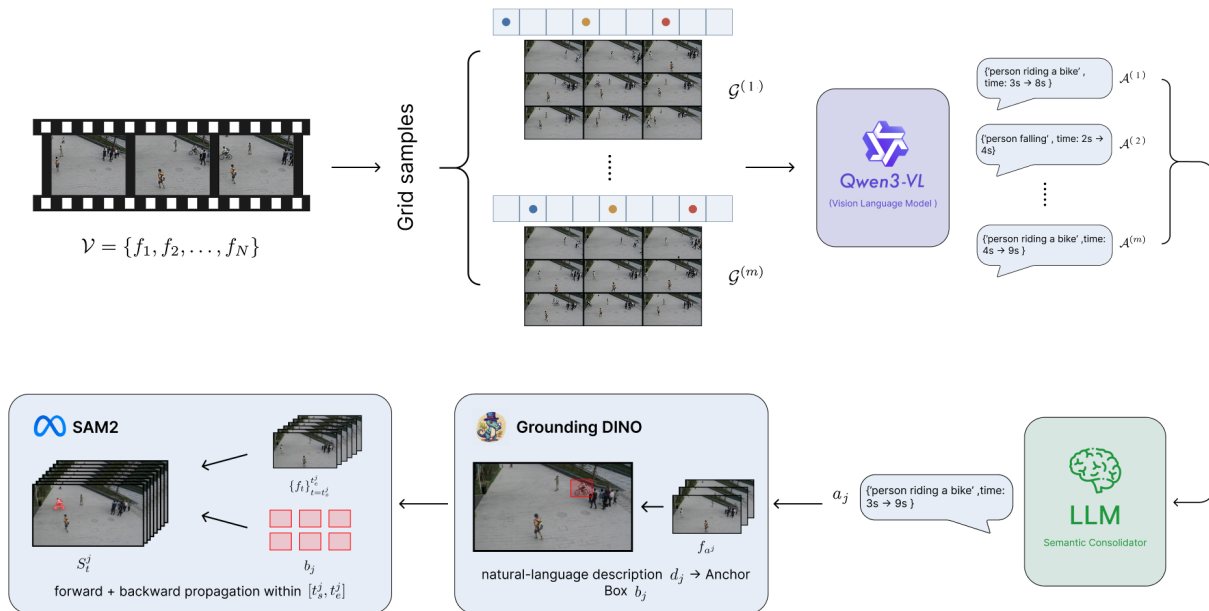


Fig. 1: Overview of the GridVAD pipeline. We convert a video into M stratified frame grids and process them by a VLM to generate anomaly proposals. A semantic consolidation step filters inconsistent proposals. The anomaly description is input to a prompt-based object detection model (Grounding DINO) to localize the anomaly, and SAM2 propagates it across frames to produce temporally consistent pixel-level anomaly masks.

prompt-tune VLMs to derive calibrated frame-level scores. Despite strong zero-shot generalization, all these methods share a common design choice: the VLM or LLM is asked to make a binary anomaly judgment, either at the frame level or the clip level. This conflates two distinct sub-problems: (1) *recognizing and describing* unusual visual content in open vocabulary, which VLMs do well, and (2) *deciding* whether that content constitutes an anomaly under the skewed class distribution of surveillance video, which VLMs and LLMs are not trained to do reliably. The result is a noisy detection signal that requires post-hoc filtering heuristics or threshold calibration to be usable.

Object-centric grounding and tracking. TAO [9] moves beyond frame-level scoring by reframing VAD as object tracking: it combines a per-object anomaly scorer, a tracking-based box refinement module, and SAM2 [20] for pixel-level segmentation. This achieves strong localization but inherits fundamental constraints: the anomaly scorer relies on pose- and depth-derived features requiring per-dataset fine-tuning, and the robustness filtering stage used by TAO depends on many hand-tuned hyperparameters. The pipeline also operates frame-by-frame, incurring $\mathcal{O}(N)$ heavy inference calls per video.

Our position. GridVAD uses a VLM to generate open-set natural-language proposals describing potential anomalous events, without requiring binary anomaly decisions. A consistency filter (SCC) retains proposals that recur across independent samplings, discarding one-off hallucinations. Purpose-built models (Grounding DINO, SAM2) then handle precise spatial and temporal localization. This decomposition requires no anomaly-domain training and no hand-tuned thresholds on the detection signal.

3 Methodology

GridVAD instantiates the *propose-ground-propagate* decomposition as a four-stage pipeline. A VLM generates free-form anomaly proposals over stratified grid representations of the clip (Secs. 3.2–3.3). A Self-

Consistency Consolidation stage filters hallucinations by retaining only proposals with cross-sampling statistical support (Sec. 3.4). Grounding DINO and SAM2 then anchor each surviving proposal spatially and propagate it temporally (Sec. 3.5). No stage is trained on anomaly data.

3.1 Problem Formulation

Let $\mathcal{V} = \{f_1, f_2, \dots, f_N\}$ be a surveillance video of N frames, where each frame $f_t \in \mathbb{R}^{H \times W \times 3}$. We define a *video anomaly* as an unexpected event that (i) occupies a contiguous temporal interval $[t_s, t_e] \subset [1, N]$, and (ii) manifests as a spatially localised region in the affected frames. The goal of fine-grained VAD is to jointly produce, *without any predefined category list or domain-specific training*:

1. a natural-language description of each detected anomaly,
2. its temporal extent $[t_s, t_e]$,
3. per-frame binary segmentation masks $\{S_t\}_{t=t_s}^{t_e}$, $S_t \in \{0, 1\}^{H \times W}$.

3.2 Stratified Grid Sampling

A clip $\mathcal{C} = \{f_s, f_{s+1}, \dots, f_e\}$ of length $L = e - s + 1$ frames is processed as follows. We fix a grid of size $K = g^2$ cells (we use $g = 3$, so $K = 9$). The clip is divided into K equal-width temporal *bins*:

$$B_k = \left[s + \frac{(k-1)L}{K}, s + \frac{kL}{K} \right), \quad k = 1, \dots, K. \quad (1)$$

For each grid sample $m \in \{1, \dots, M\}$, one frame index $i_k^{(m)} \sim \text{Uniform}(B_k)$ is drawn independently from each bin, and the K retrieved frames are tiled into a single image:

$$\mathcal{G}^{(m)} = \text{Tile}(f_{i_1^{(m)}}, \dots, f_{i_K^{(m)}}) \in \mathbb{R}^{gH \times gW \times 3}. \quad (2)$$

Stratified sampling guarantees every temporal bin is represented in each grid while the randomness ensures that the M grids show *different frames* from each bin, providing complementary views of the same clip at negligible computational cost. Our approach examines only $M \times K$ frames in total, with each of the M VLM calls processing an entire clip’s worth of temporal context in a *single forward pass*.

3.3 Open-Set Anomaly Proposal via VLM

Each grid $\mathcal{G}^{(m)}$ is passed to a VLM Φ (we use *Qwen3-VL 30B A3B* [1]) with a structured prompt \mathcal{P} requesting free-form detection, description, and temporal localisation:

$$\mathcal{A}^{(m)} = \Phi(\mathcal{G}^{(m)}, \mathcal{P}) = \{(d_j, t_s^j, t_e^j, p_j)\}_j, \quad (3)$$

where d_j is a free-form anomaly description, $[t_s^j, t_e^j]$ is the temporal interval decoded from the VLM’s reported evidence grid cells via the bin-to-frame mapping of Eq. (1), and $p_j \in [0, 1]$ is a confidence score. The VLM is given *no predefined anomaly category list*. It decides what constitutes an anomaly from first principles, enabling open-set detection of arbitrary events.

3.4 Self-Consistency Consolidation (SCC)

The M sets of proposals $\{\mathcal{A}^{(m)}\}_{m=1}^M$ are pooled into a single candidate list and passed to a second, *text-only* LLM call that acts as a semantic consolidator:

$$\mathcal{A}^* = \Phi_{\text{text}}\left(\bigcup_{m=1}^M \mathcal{A}^{(m)}, \mathcal{P}_{\text{SCC}}\right). \quad (4)$$

Each consolidated entry carries a *support count* $\sigma_j \in \{1, \dots, M\}$ recording how many of the M samplings contributed a semantically matching proposal. Only entries with $\sigma_j \geq \tau$ are retained:

$$\mathcal{A}^\dagger = \{a_j \in \mathcal{A}^* \mid \sigma_j \geq \tau\}, \quad (5)$$

where τ is the support threshold. This is the mechanism that converts a noisy proposer into a reliable detection signal: genuine anomalies, being visually consistent, recur across samplings, while hallucinations, being stochastic, do not.

The consolidation prompt instructs the model to (i) group proposals that refer to the *same object instance* across different samplings into a single entry, (ii) merge their temporal intervals by taking $t_s^* = \min_m t_s^{(m)}$ and $t_e^* = \max_m t_e^{(m)}$, and (iii) keep genuinely distinct anomalies as separate entries. This is qualitatively different from heuristic IoU-based box filtering: the VLM reasons about *semantic identity*, e.g., a vehicle moving from left-to-centre across two grids is correctly recognised as one continuous event, while a vehicle and a pedestrian in the same frames remain separate. The result is a deduplication mechanism that requires no score thresholds and no dataset-specific tuning.

Temporal precision and the role of M . Because each of the M grids samples *different* frames from the same temporal bins, independent samplings observe the anomaly at different moments within each bin of width L/K . SCC merges them by union: the consolidated interval $[t_s^*, t_e^*]$ therefore converges toward the true event boundaries as M grows, since each additional sampling provides an independently-drawn observation from the boundary bins.

3.5 Spatial Grounding and Pixel-Level Propagation

Zero-shot spatial grounding. For each surviving proposal $a_j \in \mathcal{A}^\dagger$, the natural-language description d_j is passed to Grounding DINO [13], a zero-shot open-vocabulary detector, which localises the described entity in a candidate anchor frame f_{a^j} :

$$b_j = \text{GroundingDINO}(f_{a^j}, d_j). \quad (6)$$

The anchor frame is selected as the frame with highest Grounding DINO confidence across R candidates sampled from $[t_s^j, t_e^j]$. This step bridges the gap between the VLM’s natural-language output and the pixel-level input required by SAM2, without any category-specific training.

Temporal mask propagation. Given anchor box b_j in frame f_{a^j} , we initialise a SAM2 [20] video propagation session with b_j as the spatial prompt and propagate both forward and backward within the temporal window $[t_s^j, t_e^j]$:

$$\{S_t^j\}_{t=t_s^j}^{t_e^j} = \text{SAM2}(\{f_t\}_{t=t_s^j}^{t_e^j}, b_j, a^j), \quad (7)$$

where $S_t^j \in \{0, 1\}^{H \times W}$ is the per-frame binary mask. The final anomaly mask for frame t is the union over all detected instances: $S_t = \bigcup_j S_t^j$. Propagation is restricted to the SCC-refined window $[t_s^j, t_e^j]$, so tracking errors cannot accumulate across unrelated video segments.

3.6 Full Pipeline Summary and Complexity

The complete pipeline is illustrated in Fig. 1 and summarised as:

$$\{\mathcal{G}^{(m)}\}_{m=1}^M = \text{Tile}(\mathcal{V}; M) \quad [\mathcal{O}(1) \text{ copy}] \quad (8)$$

$$\{\mathcal{A}^{(m)}\}_{m=1}^M = \Phi(\{\mathcal{G}^{(m)}\}_{m=1}^M, \mathcal{P}) \quad [M \text{ VLM forward passes}] \quad (9)$$

$$\mathcal{A}^* = \text{SCC}(\{\mathcal{A}^{(m)}\}_{m=1}^M) \quad [1 \text{ SCC pass}] \quad (10)$$

$$\mathcal{A}^\dagger = a_j \in \mathcal{A}^* \mid \sigma_j \geq \tau \quad [\text{support filter}] \quad (11)$$

$$b_j = \text{GroundingDINO}(f_{a^j}, d_j) \quad [|\mathcal{A}^*| \text{ grounding calls}] \quad (12)$$

$$S_t^j = \text{SAM2}(\{f_t\}, b_j, a^j) \quad [|\mathcal{A}^*| \text{ propagation passes}] \quad (13)$$

where $|\mathcal{A}^*|$ is the number of detected anomalies. The dominant cost is the M VLM calls (9); all subsequent steps process only the anomalous window.

4 Experiments

4.1 Experimental Setup

Datasets. We evaluate on two standard VAD benchmarks. *ShanghaiTech Campus* [14] contains 330 training and 107 test videos (480×856 pixels) across 13 campus scenes, with anomalies including fighting, robbery, and cycling in restricted areas. *UCSD Ped2* [17] contains 16 training and 12 test videos (240×360 pixels) with anomalies including cyclists, vehicles, and skateboarders operating in pedestrian zones.

Evaluation Metrics. We adopt the same evaluation protocol as *TAO* [9], spanning three complementary granularities.

Frame-level. *Frame-AUROC* measures the model’s ability to distinguish anomalous from normal frames at the video level, computed as the area under the receiver operating characteristic curve using per-frame anomaly scores. A score of 1.0 indicates perfect temporal discrimination.

Pixel-level. Here, following [9], we evaluated four pixel-level metrics. *Pixel-AUROC* assesses the model’s capability to differentiate between normal and anomalous pixels across thresholds. *Pixel-AUPRO* evaluates segmentation accuracy based on region overlap. *Pixel-AP* evaluates detection accuracy by balancing false positives and false negatives. *Pixel-F1* Combines precision and recall into a single measure.

Object-level. We report the Region-Based Detection Criterion (*RBDC*) and Track-Based Detection Criterion (*TBDC*) introduced in [7], following the same protocol as [9]. *RBDC* evaluates spatial accuracy based on intersection over union (IoU) with a threshold of α . *TBDC* assesses temporal consistency in tracking anomalous regions over frames. Both metrics are computed globally across the entire test set, as in *TAO*, rather than averaged per video.

Implementation Details. All experiments run on 4×*NVIDIA V100 32 GB GPUs*. We use *Qwen3-VL-30B-A3B-Instruct* [1] for both per-grid proposals and SCC consolidation, with support threshold $\tau=3$. Spatial grounding uses *Grounding DINO* [13] with box and text thresholds $\delta=0.05$. Pixel-level tracking uses *SAM2.1-Hiera-Tiny* [20] with a minimum mask area of 50 px². Each clip uses grid size $g=3$ ($K=9$ frames/grid) and $M=5$ independent stratified samplings. No component is fine-tuned on target datasets.

4.2 Comparison with State-of-the-Art

We compare GridVAD against representative training-based and training-free baselines on *UCSD Ped2* [17] and *ShanghaiTech Campus* [14]. Following prior work, we report pixel-level metrics (Pixel-AUROC, Pixel-AP, Pixel-AUPRO, Pixel-F1) and object-level metrics (RBDC, TBDC) where available. As shown in Tables 1–2, GridVAD achieves the highest Pixel-AUROC (77.59) on *UCSD Ped2* among all compared methods, including the partially fine-tuned *TAO*, without any task-specific training. Furthermore, it delivers competitive performance in Pixel-AP, Pixel-AUPRO, and Pixel-F1. However, the RBDC and TBDC scores remain relatively low. The gap in RBDC and TBDC reflects the proposal-recall bottleneck discussed in Section 4.6: GridVAD can only ground anomalies that the VLM first proposes in the temporal montage, while exhaustive per-frame methods like *TAO* track every object regardless. On *ShanghaiTech Campus*, this recall gap is more pronounced due to diverse scenes and subtle anomalies.

4.3 Ablation Study

Does SCC Reduce VLM Hallucinations? A core premise of GridVAD is that VLMs are noisy proposers whose raw outputs contain both genuine anomaly descriptions and confident-sounding hallucinations. Self-Consistency Consolidation (SCC) treats the VLM as a stochastic sensor and uses multiple independent samplings to separate signal from noise. We isolate the effect of SCC by comparing $M=1$ (raw VLM output, no consolidation) against $M=5$ on a 15-video subset of *ShanghaiTech Campus* [14], keeping all other pipeline components (Grounding DINO, SAM2) fixed.

Analysis. As shown in Table 3, SCC produces a clear precision-recall tradeoff. The single-pass baseline ($M=1$) achieves higher RBDC (+4.3) and TBDC (+7.3) because it retains every VLM proposal, including hallucinations, some of which happen to overlap ground-truth regions. However, these unchecked proposals also produce noisy masks: Pixel-AUROC drops by 7.3 points and Pixel-F1 by 13.8 points compared to the SCC-filtered configuration.

Table 1: Quantitative comparison on UCSD Ped2. Baseline numbers are transcribed from the TAO paper; our results are in the last row.

Method	Pixel-AUROC	Pixel-AP	Pixel-AUPRO	Pixel-F1	RBDC	TBDC
AdaCLIP (Fully fine-tuned) [4]	53.06	4.97	50.66	11.19	12.3	15.5
AnomalyCLIP (Fully fine-tuned) [33]	54.25	23.73	38.59	7.48	13.1	21.0
DDAD (Fully trained) [18]	55.87	5.61	15.12	2.67	18.01	13.29
SimpleNet (Fully trained) [16]	52.49	20.51	44.05	10.71	51.18	27.75
DRAEM (Fully trained) [30]	69.58	30.63	35.78	10.89	44.26	70.64
TAO (Partially fine-tuned) [9]	75.11	<u>50.78</u>	<u>72.97</u>	<u>64.12</u>	<u>83.6</u>	<u>93.2</u>
AdaCLIP (Zero-shot) [4]	51.02	1.32	33.98	2.61	5.8	10.6
AnomalyCLIP (Zero-shot) [33]	51.63	21.20	36.34	5.92	7.5	11.2
GridVAD (Ours, Zero-shot)	<u>77.59</u>	<u>38.53</u>	<u>66.82</u>	<u>42.09</u>	<u>38.96</u>	<u>37.70</u>

Table 2: Object-level comparison on ShanghaiTech Campus. Baseline numbers are transcribed from the TAO paper.

Method	RBDC	TBDC
OCAD [10]	20.7	44.5
AED-SSMTL [6]	43.2	84.1
HF2VAD [15]	45.4	84.5
STPT [19]	51.6	84.6
TAO [9]	<u>62.1</u>	<u>85.4</u>
GridVAD (Ours)	<u>33.32</u>	<u>14.58</u>

With $M=5$, SCC discards proposals that do not recur across independent samplings. This removes hallucinated detections and improves mask quality across all pixel-level metrics. The cost is a modest reduction in object-level recall, as some genuine but inconsistently proposed anomalies are also filtered. This trade-off directly explains the gap between pixel-level and object-level scores observed in Section 4.2: GridVAD deliberately prioritizes detection precision over exhaustive recall.

4.4 Efficiency Paradigm Comparison

We compare two VLM querying strategies on UCSD Ped2. *Uniform sampling* queries the VLM once per sampled frame (every 10 frames), providing local detail but no temporal context, with cost scaling linearly in video length. *GridVAD* (ours) batches $K=9$ frames into a spatial montage per call and issues $M=5$ passes per clip, encoding both spatial and temporal context with cost independent of video length.

As shown in Table 4, uniform sampling achieves higher absolute Frame-AUROC (0.69 vs. 0.40) by dedicating each call to a single frame, but requires $4.7\times$ more VLM calls and $2.3\times$ more wall time. Normalising by VLM calls, GridVAD is $2.7\times$ more call-efficient (Frame-AUROC per call: 0.0094 vs. 0.0035), demonstrating that structured spatial batching extracts more detection signal per model invocation than dense per-frame coverage.

4.5 Qualitative Analysis and Visualization

Fig. 2 highlights the strengths of **GridVAD**. The predicted masks are more complete and detailed, cleanly delineating object boundaries while preserving the integrity of anomalous objects. Notably, these qualitative gains are achieved in a zero-shot setting without dataset-specific fine-tuning.

4.6 Discussion and Limitations

When the proposer paradigm works. The results on UCSD Ped2 pixel-level metrics demonstrate that when the VLM correctly identifies an anomalous event, the downstream grounding and propagation stages

Table 3: Effect of SCC on ShanghaiTech Campus (15 videos). SCC improves all pixel-level metrics while reducing object-level recall, revealing a precision-recall tradeoff.

Config	Px-AUROC	Px-AP	Px-F1	RBDC	TBDC
$M=1$, no SCC	62.71	25.36	29.64	32.31	33.18
$M=5$	70.04	37.90	43.43	27.97	25.91

Table 4: Efficiency comparison on UCSD Ped2. GridVAD uses $4.7\times$ fewer VLM calls and runs $2.3\times$ faster while additionally producing dense pixel-level segmentation masks that uniform sampling cannot.

Paradigm	VLM calls	Frame-AUROC	Time (s)	Fr-AUC / call
Uniform sampling	201	0.6948	640.6	0.0035
GridVAD (Ours)	43	0.4024	276.7	0.0094

produce high-quality spatiotemporal masks. The propose-ground-propagate decomposition is effective at the localization sub-problem.

Proposal recall is the bottleneck. The primary failure mode is not mask quality but missed proposals. If the VLM does not generate a description for an anomaly in any of the M samplings, that event produces zero score across all downstream stages. The SCC ablation (Table 3) confirms this: disabling SCC ($M=1$) recovers $+4.3$ RBDC and $+7.3$ TBDC but degrades all pixel-level metrics. RBDC and TBDC measure whether GT tracks are *found*, not how well they are segmented. The current pipeline deliberately prioritizes mask quality over exhaustive recall. Improving VLM proposal recall, through better prompting, adaptive re-querying of uncertain clips, or lightweight anomaly prior injection, is the most direct path to closing the gap with trained methods without sacrificing mask precision.

Computational cost. GridVAD utilized a VLM with 3B active parameters, which is relatively expensive compared to CLIP-based methods. The per-clip budget is fixed at $M+1$ VLM calls regardless of video length, but each call is slightly heavyweight.

Clip independence. Each clip is processed independently. Anomalies that span clip boundaries may be partially missed or duplicated. Cross-clip context is currently handled only by the temporal overlap in the sliding window, not by any global reasoning.

5 Conclusion

We presented GridVAD, a training-free pipeline that repositions VLMs from direct anomaly detectors to open-set anomaly proposers within a propose-ground-propagate decomposition. By representing video clips as stratified spatial grids, GridVAD converts temporal anomaly detection into a single-pass image understanding task with a fixed per-clip VLM budget. Self-Consistency Consolidation filters hallucinations by retaining only proposals with cross-sampling support, while Grounding DINO and SAM2 provide precise spatial grounding and temporal mask propagation.

Experiments on UCSD Ped2 and ShanghaiTech Campus validate the feasibility of this decomposition: GridVAD achieves the highest Pixel-AUROC among all compared methods on UCSD Ped2, including partially fine-tuned baselines, in a fully zero-shot setting. The SCC ablation reveals a controllable precision-recall tradeoff that explains the gap between strong pixel-level and lower object-level scores. Improving VLM proposal recall, through better prompting, adaptive re-querying, or lightweight anomaly priors, is the most direct path to closing this gap without sacrificing mask quality.

References

1. Bai, S., Cai, Y., Chen, R., Chen, K., Chen, X., Cheng, Z., Deng, L., Ding, W., Gao, C., Ge, C., Ge, W., Guo, Z., Huang, Q., Huang, J., Huang, F., Hui, B., Jiang, S., Li, Z., Li, M., Li, M., Li, K., Lin, Z., Lin, J., Liu, X., Liu, J., Liu, C., Liu, Y., Liu, D., Liu, S., Lu, D., Luo, R., Lv, C., Men, R., Meng, L., Ren, X., Ren, X., Song, S., Sun, Y., Tang, J., Tu, J., Wan, J., Wang, P., Wang, P., Wang, Q., Wang, Y., Xie, T., Xu, Y., Xu,

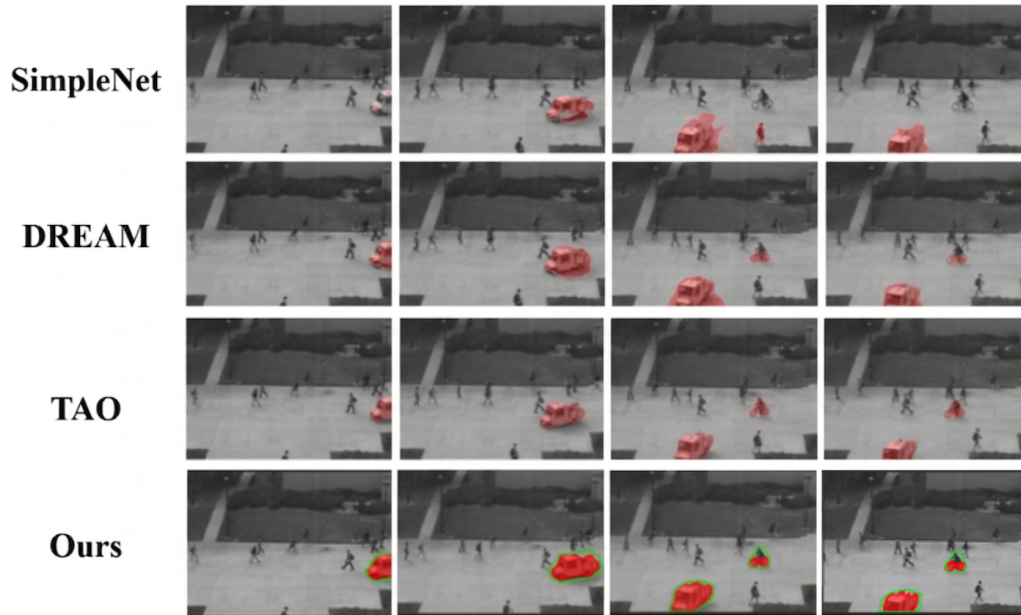


Fig. 2: Qualitative comparison with anomaly detection models adapted for video anomaly detection on the UCSD Ped2 dataset.

- H., Xu, J., Yang, Z., Yang, M., Yang, J., Yang, A., Yu, B., Zhang, F., Zhang, H., Zhang, X., Zheng, B., Zhong, H., Zhou, J., Zhou, F., Zhou, J., Zhu, Y., Zhu, K.: Qwen3-vl technical report. CoRR [abs/2511.21631](https://arxiv.org/abs/2511.21631) (2025). <https://doi.org/10.48550/ARXIV.2511.21631>, <https://doi.org/10.48550/arXiv.2511.21631>
- Bai, S., He, Z., Lei, Y., Wu, W., Zhu, C., Sun, M., Yan, J.: Traffic anomaly detection via perspective map based on spatial-temporal information matrix. In: IEEE Conference on Computer Vision and Pattern Recognition Workshops, CVPR Workshops 2019, Long Beach, CA, USA, June 16-20, 2019. pp. 117–124. Computer Vision Foundation / IEEE (2019), http://openaccess.thecvf.com/content_CVPRW_2019/html/AI_City/Bai_Traffic_Anomaly_Detection_via_Perspective_Map_based_on_Spatial-temporal_Information_CVPRW_2019_paper.html
 - Bogdoll, D., Nitsche, M., Zöllner, J.M.: Anomaly detection in autonomous driving: A survey. In: IEEE/CVF Conference on Computer Vision and Pattern Recognition Workshops, CVPR Workshops 2022, New Orleans, LA, USA, June 19-20, 2022. pp. 4487–4498. IEEE (2022). <https://doi.org/10.1109/CVPRW56347.2022.00495>, <https://doi.org/10.1109/CVPRW56347.2022.00495>
 - Cao, Y., Zhang, J., Frittoli, L., Cheng, Y., Shen, W., Boracchi, G.: Adaclip: Adapting CLIP with hybrid learnable prompts for zero-shot anomaly detection. In: Leonardis, A., Ricci, E., Roth, S., Russakovsky, O., Sattler, T., Varol, G. (eds.) Computer Vision - ECCV 2024 - 18th European Conference, Milan, Italy, September 29-October 4, 2024, Proceedings, Part XXXV. Lecture Notes in Computer Science, vol. 15093, pp. 55–72. Springer (2024). https://doi.org/10.1007/978-3-031-72761-0_4, https://doi.org/10.1007/978-3-031-72761-0_4
 - Gao, S., Yang, P., Huang, L.: SUVAD: semantic understanding based video anomaly detection using MLLM. In: 2025 IEEE International Conference on Acoustics, Speech and Signal Processing, ICASSP 2025, Hyderabad, India, April 6-11, 2025. pp. 1–5. IEEE (2025). <https://doi.org/10.1109/ICASSP49660.2025.10888431>, <https://doi.org/10.1109/ICASSP49660.2025.10888431>
 - Georgescu, M., Barbalau, A., Ionescu, R.T., Khan, F.S., Popescu, M., Shah, M.: Anomaly detection in video via self-supervised and multi-task learning. In: IEEE Conference on Computer Vision and Pattern Recognition, CVPR 2021, virtual, June 19-25, 2021. pp. 12742–12752. Computer Vision Foundation / IEEE (2021). <https://doi.org/10.1109/CVPR46437.2021.01255>, https://openaccess.thecvf.com/content/CVPR2021/html/Georgescu_Anomaly_Detection_in_Video_via_Self-Supervised_and_Multi-Task_Learning_CVPR_2021_paper.html
 - Georgescu, M.I., Barbalau, A., Ionescu, R.T., Khan, F.S., Popescu, M., Shah, M.: A background-agnostic framework with adversarial training for abnormal event detection in video. IEEE Trans. Pattern Anal. Mach. Intell. **44**(9), 4505–4523 (2022). <https://doi.org/10.1109/TPAMI.2021.3074805>, <https://doi.org/10.1109/TPAMI.2021.3074805>

8. Gong, D., Liu, L., Le, V., Saha, B., Mansour, M.R., Venkatesh, S., van den Hengel, A.: Memorizing normality to detect anomaly: Memory-augmented deep autoencoder for unsupervised anomaly detection. In: 2019 IEEE/CVF International Conference on Computer Vision, ICCV 2019, Seoul, Korea (South), October 27 - November 2, 2019. pp. 1705–1714. IEEE (2019). <https://doi.org/10.1109/ICCV.2019.00179>, <https://doi.org/10.1109/ICCV.2019.00179>
9. Huang, Y., Li, C., Zhang, H., Lin, Z., Lin, Y., Liu, H., Li, W., Liu, X., Gao, J., Huang, Y., Ding, X., Yuan, Y.: Track any anomalous object: A granular video anomaly detection pipeline. In: IEEE/CVF Conference on Computer Vision and Pattern Recognition, CVPR 2025, Nashville, TN, USA, June 11-15, 2025. pp. 8689–8699. Computer Vision Foundation / IEEE (2025). <https://doi.org/10.1109/CVPR52734.2025.00812>, https://openaccess.thecvf.com/content/CVPR2025/html/Huang_Track_Any_Anomalous_ObjectA_Granular_Video_Anomaly_Detection_Pipeline_CVPR_2025_paper.html
10. Ionescu, R.T., Khan, F.S., Georgescu, M., Shao, L.: Object-centric auto-encoders and dummy anomalies for abnormal event detection in video. In: IEEE Conference on Computer Vision and Pattern Recognition, CVPR 2019, Long Beach, CA, USA, June 16-20, 2019. pp. 7842–7851. Computer Vision Foundation / IEEE (2019). <https://doi.org/10.1109/CVPR.2019.00803>, http://openaccess.thecvf.com/content_CVPR_2019/html/Ionescu_Object-Centric_Auto-Encoders_and_Dummy_Anomalies_for_Abnormal_Event_Detection_in_CVPR_2019_paper.html
11. Li, G., Cai, G., Zeng, X., Zhao, R.: Scale-aware spatio-temporal relation learning for video anomaly detection. In: Avidan, S., Brostow, G.J., Cissé, M., Farinella, G.M., Hassner, T. (eds.) Computer Vision - ECCV 2022 - 17th European Conference, Tel Aviv, Israel, October 23-27, 2022, Proceedings, Part IV. Lecture Notes in Computer Science, vol. 13664, pp. 333–350. Springer (2022). https://doi.org/10.1007/978-3-031-19772-7_20
12. Liu, K., Ma, H.: Exploring background-bias for anomaly detection in surveillance videos. In: Amsaleg, L., Huet, B., Larson, M.A., Gravier, G., Hung, H., Ngo, C., Ooi, W.T. (eds.) Proceedings of the 27th ACM International Conference on Multimedia, MM 2019, Nice, France, October 21-25, 2019. pp. 1490–1499. ACM (2019). <https://doi.org/10.1145/3343031.3350998>, <https://doi.org/10.1145/3343031.3350998>
13. Liu, S., Zeng, Z., Ren, T., Li, F., Zhang, H., Yang, J., Jiang, Q., Li, C., Yang, J., Su, H., Zhu, J., Zhang, L.: Grounding DINO: marrying DINO with grounded pre-training for open-set object detection. In: Leonardis, A., Ricci, E., Roth, S., Russakovsky, O., Sattler, T., Varol, G. (eds.) Computer Vision - ECCV 2024 - 18th European Conference, Milan, Italy, September 29-October 4, 2024, Proceedings, Part XLVII. Lecture Notes in Computer Science, vol. 15105, pp. 38–55. Springer (2024). https://doi.org/10.1007/978-3-031-72970-6_3, https://doi.org/10.1007/978-3-031-72970-6_3
14. Liu, W., Luo, W., Lian, D., Gao, S.: Future frame prediction for anomaly detection - A new baseline. In: 2018 IEEE Conference on Computer Vision and Pattern Recognition, CVPR 2018, Salt Lake City, UT, USA, June 18-22, 2018. pp. 6536–6545. Computer Vision Foundation / IEEE Computer Society (2018). <https://doi.org/10.1109/CVPR.2018.00684>, http://openaccess.thecvf.com/content_cvpr_2018/html/Liu_Future_Frame_Prediction_CVPR_2018_paper.html
15. Liu, Z., Nie, Y., Long, C., Zhang, Q., Li, G.: A hybrid video anomaly detection framework via memory-augmented flow reconstruction and flow-guided frame prediction. In: 2021 IEEE/CVF International Conference on Computer Vision, ICCV 2021, Montreal, QC, Canada, October 10-17, 2021. pp. 13568–13577. IEEE (2021). <https://doi.org/10.1109/ICCV48922.2021.01333>, <https://doi.org/10.1109/ICCV48922.2021.01333>
16. Liu, Z., Zhou, Y., Xu, Y., Wang, Z.: Simplenet: A simple network for image anomaly detection and localization. CoRR **abs/2303.15140** (2023). <https://doi.org/10.48550/ARXIV.2303.15140>, <https://doi.org/10.48550/arXiv.2303.15140>
17. Mahadevan, V., Li, W., Bhalodia, V., Vasconcelos, N.: Anomaly detection in crowded scenes. In: The Twenty-Third IEEE Conference on Computer Vision and Pattern Recognition, CVPR 2010, San Francisco, CA, USA, 13-18 June 2010. pp. 1975–1981. IEEE Computer Society (2010). <https://doi.org/10.1109/CVPR.2010.5539872>, <https://doi.org/10.1109/CVPR.2010.5539872>
18. Mousakhan, A., Brox, T., Tayyub, J.: Anomaly detection with conditioned denoising diffusion models. CoRR **abs/2305.15956** (2023). <https://doi.org/10.48550/ARXIV.2305.15956>, <https://doi.org/10.48550/arXiv.2305.15956>
19. Naji, Y., Setkov, A., Loesch, A., Gouiffès, M., Audigier, R.: Spatio-temporal predictive tasks for abnormal event detection in videos. In: 18th IEEE International Conference on Advanced Video and Signal Based Surveillance, AVSS 2022, Madrid, Spain, November 29 - Dec. 2, 2022. pp. 1–8. IEEE (2022). <https://doi.org/10.1109/AVSS56176.2022.9959669>, <https://doi.org/10.1109/AVSS56176.2022.9959669>
20. Ravi, N., Gabeur, V., Hu, Y., Hu, R., Ryali, C., Ma, T., Khedr, H., Rädle, R., Rolland, C., Gustafson, L., Mintun, E., Pan, J., Alwala, K.V., Carion, N., Wu, C., Girshick, R.B., Dollár, P., Feichtenhofer, C.: SAM 2: Segment anything in images and videos. In: The Thirteenth International Conference on Learning Representations, ICLR 2025, Singapore, April 24-28, 2025. OpenReview.net (2025), <https://openreview.net/forum?id=Ha6RTeWMD0>

21. Reiss, T., Hoshen, Y.: An attribute-based method for video anomaly detection. *Trans. Mach. Learn. Res.* **2025** (2025), <https://openreview.net/forum?id=XL1N6iLr0G>
22. Roth, K., Pemula, L., Zepeda, J., Schölkopf, B., Brox, T., Gehler, P.V.: Towards total recall in industrial anomaly detection. In: *IEEE/CVF Conference on Computer Vision and Pattern Recognition, CVPR 2022, New Orleans, LA, USA, June 18-24, 2022*. pp. 14298–14308. IEEE (2022). <https://doi.org/10.1109/CVPR52688.2022.01392>, <https://doi.org/10.1109/CVPR52688.2022.01392>
23. Sultani, W., Chen, C., Shah, M.: Real-world anomaly detection in surveillance videos. In: *2018 IEEE Conference on Computer Vision and Pattern Recognition, CVPR 2018, Salt Lake City, UT, USA, June 18-22, 2018*. pp. 6479–6488. Computer Vision Foundation / IEEE Computer Society (2018). <https://doi.org/10.1109/CVPR.2018.00678>, http://openaccess.thecvf.com/content_cvpr_2018/html/Sultani_Real-World_Anomaly_Detection_CVPR_2018_paper.html
24. Sun, S., Gong, X.: Hierarchical semantic contrast for scene-aware video anomaly detection. In: *IEEE/CVF Conference on Computer Vision and Pattern Recognition, CVPR 2023, Vancouver, BC, Canada, June 17-24, 2023*. pp. 22846–22856. IEEE (2023). <https://doi.org/10.1109/CVPR52729.2023.02188>, <https://doi.org/10.1109/CVPR52729.2023.02188>
25. Wang, G., Yuan, X., Zheng, A., Hsu, H., Hwang, J.: Anomaly candidate identification and starting time estimation of vehicles from traffic videos. In: *IEEE Conference on Computer Vision and Pattern Recognition Workshops, CVPR Workshops 2019, Long Beach, CA, USA, June 16-20, 2019*. pp. 382–390. Computer Vision Foundation / IEEE (2019), http://openaccess.thecvf.com/content_CVPRW_2019/html/AI-City/Wang_Anomaly_Candidate_Identification_and_Starting_Time_Estimation_of_Vehicles_from_CVPRW_2019_paper.html
26. Wu, P., Liu, J.: Learning causal temporal relation and feature discrimination for anomaly detection. *IEEE Trans. Image Process.* **30**, 3513–3527 (2021). <https://doi.org/10.1109/TIP.2021.3062192>, <https://doi.org/10.1109/TIP.2021.3062192>
27. Yang, Z., Liu, J., Wu, Z., Wu, P., Liu, X.: Video event restoration based on keyframes for video anomaly detection. In: *IEEE/CVF Conference on Computer Vision and Pattern Recognition, CVPR 2023, Vancouver, BC, Canada, June 17-24, 2023*. pp. 14592–14601. IEEE (2023). <https://doi.org/10.1109/CVPR52729.2023.01402>, <https://doi.org/10.1109/CVPR52729.2023.01402>
28. Ye, M., Liu, W., He, P.: VERA: explainable video anomaly detection via verbalized learning of vision-language models. In: *IEEE/CVF Conference on Computer Vision and Pattern Recognition, CVPR 2025, Nashville, TN, USA, June 11-15, 2025*. pp. 8679–8688. Computer Vision Foundation / IEEE (2025). <https://doi.org/10.1109/CVPR52734.2025.00811>, https://openaccess.thecvf.com/content/CVPR2025/html/Ye_VERA_Explainable_Video_Anomaly_Detection_via_Verbalized_Learning_of_Vision-Language_CVPR_2025_paper.html
29. Zarella, L., Menapace, W., Mancini, M., Wang, Y., Ricci, E.: Harnessing large language models for training-free video anomaly detection. In: *IEEE/CVF Conference on Computer Vision and Pattern Recognition, CVPR 2024, Seattle, WA, USA, June 16-22, 2024*. pp. 18527–18536. IEEE (2024). <https://doi.org/10.1109/CVPR52733.2024.01753>, <https://doi.org/10.1109/CVPR52733.2024.01753>
30. Zavrtnik, V., Kristan, M., Skocaj, D.: Dræm - A discriminatively trained reconstruction embedding for surface anomaly detection. In: *2021 IEEE/CVF International Conference on Computer Vision, ICCV 2021, Montreal, QC, Canada, October 10-17, 2021*. pp. 8310–8319. IEEE (2021). <https://doi.org/10.1109/ICCV48922.2021.00822>, <https://doi.org/10.1109/ICCV48922.2021.00822>
31. Zhang, H., Xu, X., Wang, X., Zuo, J., Han, C., Huang, X., Gao, C., Wang, Y., Sang, N.: Holmes-vad: Towards unbiased and explainable video anomaly detection via multi-modal LLM. *CoRR abs/2406.12235* (2024). <https://doi.org/10.48550/ARXIV.2406.12235>, <https://doi.org/10.48550/arXiv.2406.12235>
32. Zhou, H., Yu, J., Yang, W.: Dual memory units with uncertainty regulation for weakly supervised video anomaly detection. In: Williams, B., Chen, Y., Neville, J. (eds.) *Thirty-Seventh AAAI Conference on Artificial Intelligence, AAAI 2023, Thirty-Fifth Conference on Innovative Applications of Artificial Intelligence, IAAI 2023, Thirteenth Symposium on Educational Advances in Artificial Intelligence, EAAI 2023, Washington, DC, USA, February 7-14, 2023*. pp. 3769–3777. AAAI Press (2023). <https://doi.org/10.1609/AAAI.V37I3.25489>, <https://doi.org/10.1609/aaai.v37i3.25489>
33. Zhou, Q., Pang, G., Tian, Y., He, S., Chen, J.: Anomalyclip: Object-agnostic prompt learning for zero-shot anomaly detection. *CoRR abs/2310.18961* (2023). <https://doi.org/10.48550/ARXIV.2310.18961>, <https://doi.org/10.48550/arXiv.2310.18961>